

See discussions, stats, and author profiles for this publication at: <https://www.researchgate.net/publication/278340070>

Visible Light Mediated Controlled Radical Polymerization in the Absence of Exogenous Radical Sources or Catalysts

ARTICLE *in* MACROMOLECULES · JUNE 2015

Impact Factor: 5.8 · DOI: 10.1021/acs.macromol.5b00965

CITATIONS

7

READS

52

5 AUTHORS, INCLUDING:



Thomas Mckenzie

University of Melbourne

5 PUBLICATIONS 16 CITATIONS

SEE PROFILE



Qiang Fu

University of Melbourne

28 PUBLICATIONS 153 CITATIONS

SEE PROFILE



Edgar Wong

University of New South Wales

40 PUBLICATIONS 434 CITATIONS

SEE PROFILE

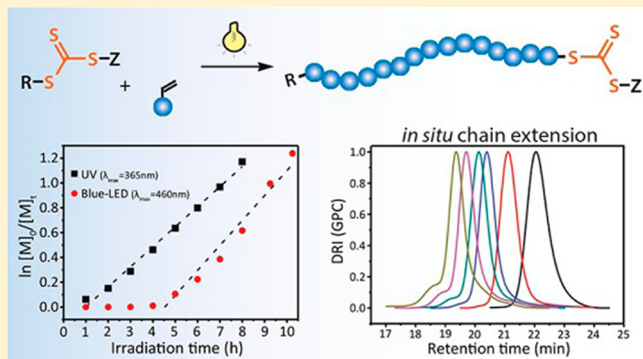
Visible Light Mediated Controlled Radical Polymerization in the Absence of Exogenous Radical Sources or Catalysts

Thomas G. McKenzie, Qiang Fu, Edgar H. H. Wong, Dave E. Dunstan, and Greg G. Qiao*

Department of Chemical and Biomolecular Engineering, The University of Melbourne, Parkville, Victoria 3010, Australia

S Supporting Information

ABSTRACT: The application of external stimuli such as light to induce controlled radical polymerization reactions has important implications in the field of materials science. In this study, the photoactivation of trithiocarbonates (TTCs) (i.e., conventional RAFT agents) by visible light (~ 460 nm) is investigated, and the ability of TTCs to control radical polymerization under visible light in the complete absence of exogenous photoinitiators or catalysts is demonstrated for the first time. By selectively exciting the spin-forbidden $n \rightarrow \pi^*$ electronic transition, polyacrylates and polyacrylamides of low dispersity and high end group fidelity were obtained. In addition, this approach allows for the efficient synthesis of well-defined linear, (multi)block, and network (co)polymers. This study demonstrates the versatility of our strategy to generate polymers with controllable properties by visible light, which may be highly useful for applications such as surface patterning.



INTRODUCTION

Reversible deactivation radical polymerization (RDRP) techniques such as atom-transfer radical polymerization (ATRP),^{1–3} single electron-transfer living radical polymerization (SET-LRP),^{4–6} nitroxide mediated polymerization (NMP),^{7,8} and reversible addition–fragmentation chain transfer (RAFT) polymerization^{9,10} are now commonly employed for the preparation of advanced polymer nanomaterials for many high-end applications.^{11,12} Recently, significant interest has been devoted toward exerting control over RDRP reactions through the application of an external stimulus.^{13–15} From the multitude of external stimuli available, light is considered the most ideal due to its inherent spatiotemporal characteristics, relative ease of operation, environmentally benign nature, and availability of cheap commercial light sources.¹⁶ For example, Hawker et al. have shown that a visible light absorbing Ir-complex photocatalyst can induce an ATRP-like radical polymerization of (meth)acrylate monomers via light mediated activation/deactivation of terminal carbon–halogen bonds.^{17,18} This technique was subsequently utilized to create photopatterned surfaces via a grafting-from approach, generating unique chemical patterns and gradients while clearly demonstrating the advantages of photocontrolled polymerization.^{19,20} Many other photocontrolled radical polymerization systems have since been reported, primarily as derivatives of the above-mentioned RDRP techniques^{14,21–29} with each offering a particular set of associated benefits and limitations including the type of catalyst used (metal or organic), the range of polymerizable monomers, and the wavelength of irradiation required for activation.^{16,30,31}

It has been previously established that ultraviolet (UV) light can induce radical polymerizations through the photochemical activation of thio-containing compounds.^{32–38} For thiocarbonylthio compounds, UV irradiation can lead to fragmentation of the weak C–S bond adjacent to the photoactive C=S moiety,^{39,40} resulting in the generation of a reactive carbon-centered radical as well as a more stable sulfur-centered radical. The carbon-centered radical can react with vinyl monomer species or with unfragmented thiocarbonylthio compounds via degenerative transfer to initiate a radical polymerization process.³³ Once initiated, the polymerization can proceed via a degenerative chain transfer (i.e., RAFT) mechanism or by direct dissociation–recombination of the generated radical pair. All thiocarbonyl-containing molecules share similar absorption characteristics as a result of the electronic transitions available to the C=S double bond.⁴¹ These are analogous to the more extensively studied carbonyl (C=O) electronic transitions but tend to be shifted to slightly lower energies (i.e., longer wavelengths) due to the lower electronegativity—or “softer” nature—of the sulfur atom (Figure 1 and Figure S1, Supporting Information). A large broad absorption band at ~ 320 nm is ascribed to the spin-allowed $\pi \rightarrow \pi^*$ electronic transition. When irradiating with light in this wavelength range (i.e., UV, $\lambda < 380$ nm), the compound can be photochemically excited to a higher energy state from which several transformations and reactions can occur.⁴² However, unlike the photophysical

Received: May 6, 2015

Revised: May 26, 2015

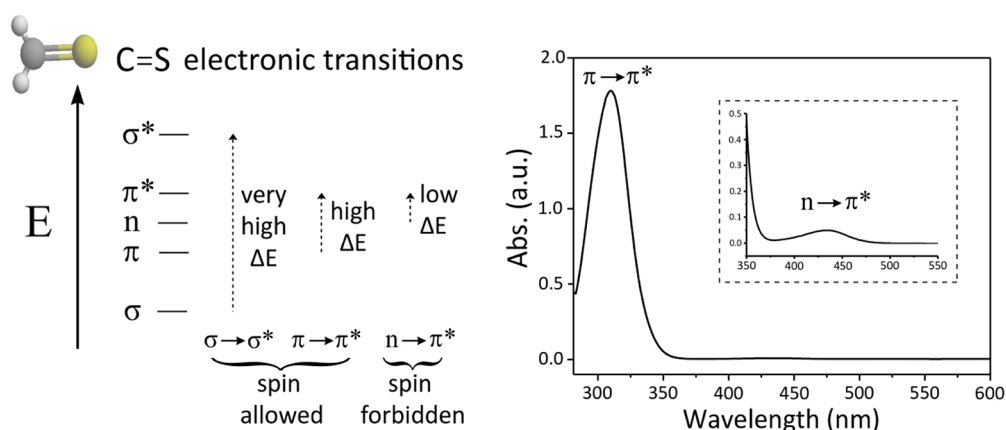


Figure 1. Simplified electronic energy level diagram for thiocarbonyl compounds and representative UV-vis absorption spectrum of a trithiocarbonate compound (TTC-1, 0.1 mM in toluene). Inset shows the spin-forbidden $n \rightarrow \pi^*$ absorption band.

properties of carbonyl compounds (i.e., $C=O$ containing), whose absorption bands typically fall exclusively in the UV region of the electromagnetic spectrum, the spin-forbidden $n \rightarrow \pi^*$ electronic transition of thiocarbonyl compounds has an absorption energy that falls in the visible region ($\lambda_{\max, n \rightarrow \pi^*} = 400\text{--}550\text{ nm}$).⁴¹ This absorption band is what gives thiocarbonyl compounds their distinctive color.⁴⁰ Because of this secondary absorption band, thiocarbonyl species can be excited by visible light,^{40,41,43–47} but this property has been somewhat overlooked as a means toward photochemical transformations, particularly in the field of polymer science where the addition of exogenous photoinitiators or photocatalysts has been the preferred choice for photoactivation.^{28,46–53}

Visible light mediated photochemistry has many advantages over other, higher energy irradiation sources (e.g., UV or γ -radiation).^{54–56} Given the abundance of natural visible light reaching the Earth's surface from the Sun every day, harnessing this energy to drive chemical reactions has been a long held goal for chemists worldwide.⁵⁷ Additionally, because many organic molecules absorb UV light, activation via UV irradiation increases the probability of unwanted side reactions or degradation of reagents,⁵⁶ thereby limiting the yield of the desired product. Furthermore, visible light is much safer for use in biological applications as it causes minimal damage to cells or soft tissue compared with UV radiation. Therefore, photochemical transformations that proceed exclusively through visible light mediated activation are highly desirable.

In this study, we demonstrate that visible light irradiation of trithiocarbonates (TTCs) (i.e., RAFT agents) can effectively induce photocontrolled radical polymerization processes without the aid of any additional radical (photo)initiators or catalysts. This simplistic approach enables the efficient preparation of well-defined, high molecular weight polyacrylates and polyacrylamides with excellent retention of α,ω -end-groups even at high monomer conversions, thus allowing for the efficient formation of (multi)block copolymers of low dispersity in a one-pot fashion. The versatility of this reaction is also demonstrated through the synthesis of a variety of linear polymers in a range of solvents of varying polarity, including water. To the best of our knowledge, there are no reports in the literature detailing the direct activation of trithiocarbonates with visible light.

EXPERIMENTAL SECTION

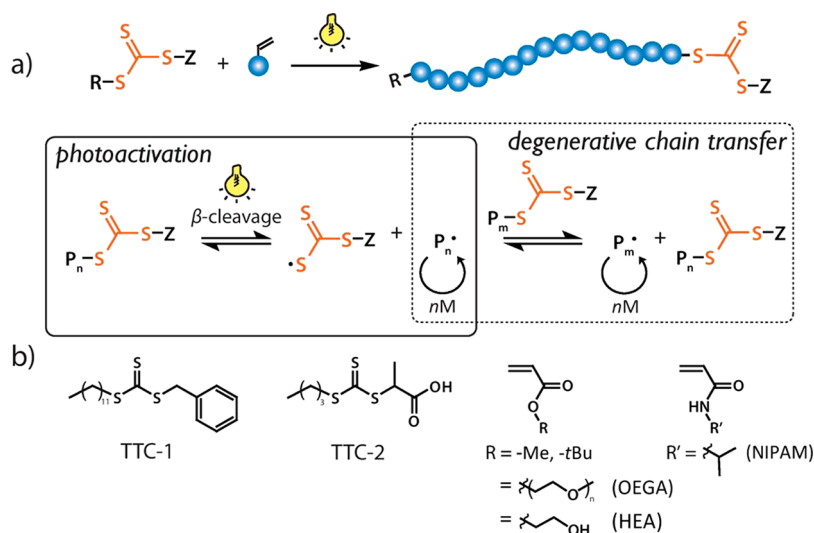
Materials. Monomers methyl acrylate (MA, Aldrich, 99%), 2-hydroxyethyl acrylate (HEA, 96%, Aldrich), oligo(ethylene glycol) ethyl ether acrylate (OEGA, $M_w = 480\text{ g mol}^{-1}$, >90%, Aldrich), *tert*-butyl acrylate (*t*BA, 98%, Aldrich), and ethylene glycol diacrylate (EGDA, Aldrich, 90%, technical grade) were passed over basic alumina to remove inhibitors prior to use. *N*-Isopropylacrylamide (NIPAM, >97%, Aldrich) was recrystallized twice from hexane to remove inhibitors. Benzyl dodecyl carbonotrithioate (TTC-1) was synthesized as previously reported.⁵⁸ 2-(((Butylthio)carbonothiolyl)thio)propanoic acid (TTC-2) was received from Dulux Group Australia and used as received. Dimethyl sulfoxide (DMSO), dimethylformamide (DMF), acetone, toluene, and tetrahydrofuran (THF) were purchased from Chem-Supply Pty Ltd. and used as received. Dioxane (Aldrich, 99.8%, anhydrous) was used as received. Deuterated chloroform ($CDCl_3$, 99.9%) was purchased from Cambridge Isotope Laboratories Inc. The LED light source used for all experiments was a commercial strip lighting (300 LEDs, 4.8 W) wound around the inside of a beaker. The LED light emission spectrum ($\lambda_{\max} \sim 460\text{ nm}$) was measured using a Maya 2000Pro spectrometer fitted with optical fiber (OceanOptics 100UV). The UV lamp used for UV-activated polymerizations was a UVP 95-0045-04 Model XX-20BLB Blak-Ray UV bench lamp, 20 W, with $\lambda_{\max} = 365\text{ nm}$.

Characterization. *Nuclear Magnetic Resonance (NMR) Spectroscopy.* 1H NMR spectroscopy was conducted on a Varian Unity 400 MHz spectrometer operating at 400 MHz, using the deuterated solvent ($CDCl_3$) as reference and a sample concentration of approximately 10 mg mL^{-1} .

Gel-Permeation Chromatography (GPC). GPC using THF as an eluent was carried out on a Shimadzu liquid chromatography system equipped with a Wyatt OPTILAB DSP interferometric refractometer (690 nm) and Shimadzu SPD-10AVP UV-vis detector using three Phenomenex Phenogel columns (500, 104, and 106 Å porosity; $5\text{ }\mu\text{m}$ bead size) operating at $45\text{ }^\circ\text{C}$. The flow rate was set at 1 mL min^{-1} . The molecular weights were determined based on monodisperse polystyrene standards. When DMF was used as an eluent, the GPC analysis was conducted on a Shimadzu liquid chromatography system equipped with a Shimadzu RID-10 refractometer ($\lambda = 633\text{ nm}$) and Shimadzu SPD-20A UV-vis detector using three identical Jordi columns ($5\text{ }\mu\text{m}$ bead size, Jordi gel fluorinated DVB mixed bed) in series operating at $70\text{ }^\circ\text{C}$. DMF with 0.05 mol L^{-1} LiBr (>99%, Aldrich) was employed as the mobile phase at a flow rate of 1 mL min^{-1} . The system was calibrated using polystyrene standards. All samples were filtered through $0.45\text{ }\mu\text{m}$ nylon filters prior to injection.

UV-vis Spectroscopy. UV-vis absorbance spectra were obtained using Shimadzu UV-1800 spectrophotometer and UVProbe software package. The wavelength range of 290–600 nm was selected with a slow scan speed and sampling interval of 1 nm.

Scheme 1. (a) Photoactivated Polymerization of Vinyl Monomers Employing Trithiocarbonate as the Sole Photoactive Compound;^a (b) Chemical Structures of Trithiocarbonates (TTC-1 and TTC-2) and Monomers Investigated in This Study



^aRadical generation (i.e. activation) occurs via β -cleavage (C–S bond fragmentation) of photoexcited thiocarbonyl, after which chain propagation can be controlled via degenerative chain transfer and/or reversible chain termination.

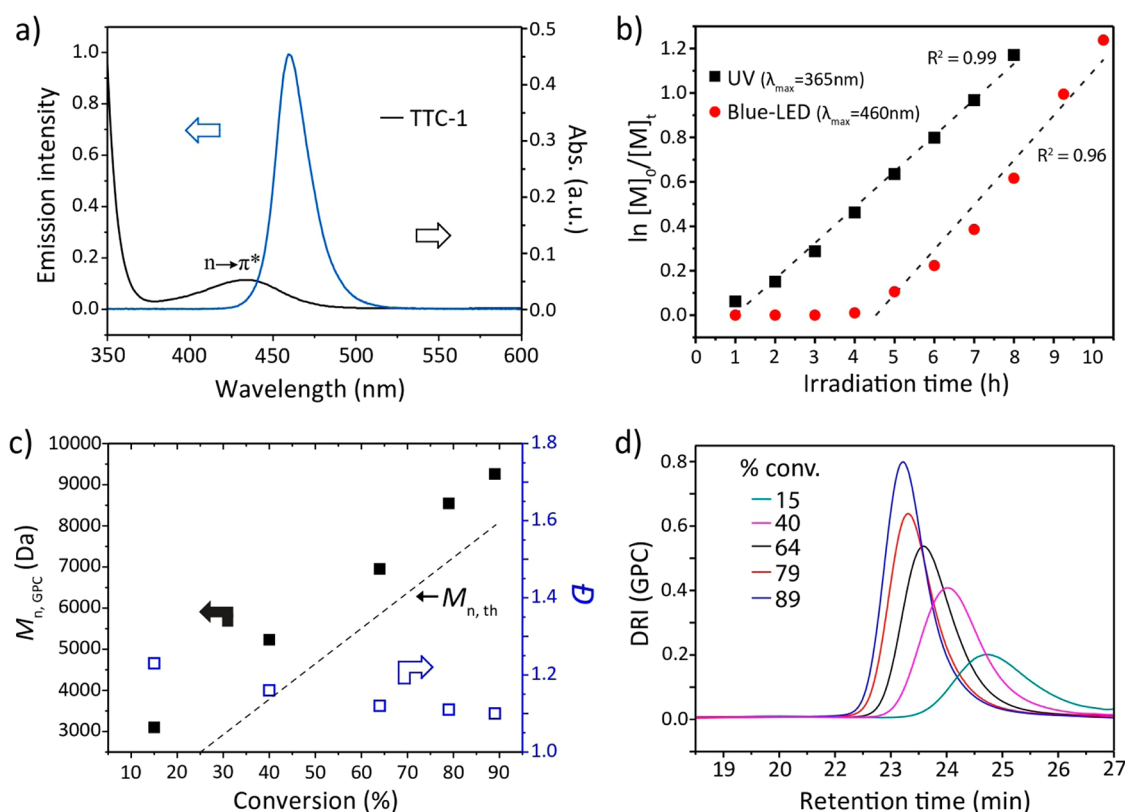


Figure 2. (a) Blue LED light source emission characterization and UV–vis absorption spectrum of TTC-1 showing emission-absorption overlap. (b) Kinetic plots for photopolymerization of MA using UV irradiation (black squares) and visible light (red circles). (c) Linear increase of molecular weight with monomer conversion for visible light mediated photopolymerization. (d) GPC differential refractive index (DRI) chromatograms of growing polymer chain.

Methods. Synthesis of Linear Homopolymers under UV Light. In a typical experiment, a 25 mL Schlenk tube was charged with MA (1.5 mL, 16.7 mmol), TTC-1 (61 mg, 0.167 mmol), and DMSO (50 vol % with respect to monomer), [MA]:[TTC] = 100:1. The reaction mixture was degassed by three freeze–pump–thaw cycles and then backfilled with argon. The flask was placed ca. 3 cm from the UV light source ($\lambda_{\max} = 365$ nm, 20 W), and the photoreactor was covered with

black plastic to block out external light sources. The UV lamp was then switched “on” to mark the start of the reaction, and the reaction mixture was left to stir at room temperature for designated time intervals. For kinetic experiments, samples were taken periodically via degassed syringe and immediately diluted with CDCl_3 and THF for NMR and GPC analysis, respectively. Monomer conversion was estimated from ^1H NMR by comparing the integrals of the peaks

Table 1. Experimental Conditions and Characterization Data for PMA Homopolymers Synthesized via UV and Visible Light Mediated Photopolymerization

entry	light ^a	TTC ^b	solvent	$[M]_0/[TTC]_0$	t (h)	% conv ^c	$M_{n,th}$ ^d (Da)	$M_{n,GPC}$ ^e (Da)	\bar{D} ^e
1	thermal/dark	1	DMSO	100	24	0			
2	UV	1	DMSO	100	16	92	8290	12280	1.12
3	UV	2	DMSO	100	24	96	8500	9040	1.08
4	UV		DMSO	n/a	16	gel			
5	Vis	1	DMSO	100	16	92	8290	10670	1.07
6	Vis	2	DMSO	100	16	95	8420	9330	1.06
7	Vis		DMSO	100	24	0			

^a“Vis” refers to irradiation via blue LED photoreactor. ^bSee Figure 1 for TTC molecular structures. ^cObtained by ¹H NMR characterization. ^dCalculated via the equation $M_n = [M]_0/[TTC]_0 \times M_w^M \times \% \text{ conv} + M_w^{TTC}$, where $[M]_0/[TTC]_0$, M_w^M , % conv, and M_w^{TTC} correspond to the initial monomer and trithiocarbonate concentrations, molar mass of monomer, monomer conversion, and molar mass of trithiocarbonate, respectively. ^e M_n and \bar{D} values determined by GPC analysis based on polystyrene standards.

corresponding to the polymer backbone ($\delta_H \sim 1.5$ ppm, t, 2H, $-\text{[CH}_2\text{--CH]}_n-$ and $\delta_H \sim 2.2$ ppm, s, 1H, $-\text{[CH}_2\text{--CH]}_n-$) to those corresponding to the unsaturated acrylate/acrylamide double bond ($\delta_H \sim 5.7$ ppm, s, 1H, $\text{H}_2\text{C=CH}$).

Synthesis of Linear Homopolymers under Visible Light. Reactions were carried out in the same fashion as for UV-activated polymerizations, with the only exception being the irradiation source is a photoreactor constructed from a blue LED light strip (300 LEDs, 4.8 W, $\lambda_{\text{max}} = 460$ nm) wound around the inside of a beaker and connected to a variable voltage potentiostat that was set at 12 V for all experiments.

RESULTS AND DISCUSSION

Photocontrolled Radical Polymerization via Visible Light Irradiation. Visible light activation has long been considered a highly desirable feature to drive chemical transformations.^{54,56,57} Herein, we demonstrate the application of a visible light source to selectively excite the $n \rightarrow \pi^*$ thiocarbonyl absorption band—i.e., the lower energy activation pathway (Figure 1)—to induce photocontrolled radical polymerization processes (Scheme 1). A visible light photoreactor was constructed consisting of a blue LED strip light (300 LEDs, 4.8 W output) wound around the inside of a beaker (Figure S2). The peak emission (λ_{max}) from this light source was measured to be ~ 460 nm, displaying clear emission-absorption overlap with the $n \rightarrow \pi^*$ band of TTC-1, while avoiding stimulation of the $\pi \rightarrow \pi^*$ absorption band (Figure 2a). The visible light mediated photopolymerizations were conducted as follows. A model trithiocarbonate (benzylododecyl trithiocarbonate (TTC-1), 1 equiv) and vinyl monomer (methyl acrylate (MA), 100 equiv) were dissolved in a solvent (dimethyl sulfoxide (DMSO), 50% v/v), followed by oxygen removal via three consecutive freeze–pump–thaw cycles. The reaction mixture was then backfilled with argon, sealed, and placed in the photoreactor above a magnetic stirrer plate. The light source was turned on to mark the start of the reaction. Samples were extracted periodically to monitor monomer conversion and molecular weight evolution via ¹H NMR and GPC analysis, respectively. After an induction period of ca. 4 h, the polymerization was found to proceed in a pseudo-“living” fashion, where linear trends were observed for the semi-logarithmic plot of monomer conversion versus irradiation time and the evolution of molecular weight with monomer conversion (Figure 2b,c).

We also carried out UV-activated photocontrolled radical polymerizations to compare the photoactivity of the employed TTC compounds. Using a UV lamp with peak emission wavelength (λ_{max}) of 365 nm, we irradiated a degassed reaction

mixture containing TTC-1 (1 equiv), MA (100 equiv), and DMSO (50% v/v), extracting aliquots periodically for ¹H NMR and GPC analysis (Figure S3). The increase in monomer conversion over the course of irradiation time indicates a pseudo-“living” polymerization process following a much shorter induction period (<1 h) (Figure 2b and Figure S3a). The observed number-averaged molecular weights (M_n) are in close agreement with theoretical values, and the dispersity (\bar{D}) remained low throughout (<1.26) (Figure S3b). In addition, the chain-end fidelity (or “livingness”) at (near) full monomer conversion is shown to be extremely high, as demonstrated by two successful *in situ* chain extensions in one-pot via the sequential addition of fresh monomer (MA) (Figure S3c,d). These results, which confirmed the photoactivity of TTC-1 in the UV region, agree well with other recent investigations of similar polymerization systems^{35–37} and provide further evidence to the claim that suppression of photolysis of the thiocarbonylthio moiety under UV irradiation may not be essential to achieve a well-controlled polymerization as has previously been assumed.⁴²

Surprisingly, despite the $n \rightarrow \pi^*$ absorption being weaker compared to the $\pi \rightarrow \pi^*$ transition, the visible light system proceeded with a rate almost identical to that of the UV-activated process after their respective induction periods (Figure 2b). However, it should be noted that the rate of photocontrolled radical polymerizations has been shown to be modulated by the intensity of incident light.^{35–37} Further investigation into the exact rates of polymerization as a function of irradiation intensity for both UV and visible light mediated pathways is currently being conducted in our lab. The molecular weight distributions of the resultant poly(methyl acrylate) (PMA) at different monomer conversions were monomodal and narrowly dispersed, with \bar{D} values ≤ 1.23 (Figure 2c,d). In addition, the M_n values of the polymers determined by GPC analysis are in close agreement with their calculated theoretical values, with differences ascribed to the different hydrodynamic volumes of PMA compared to the polystyrene standards used for calibration. The polymerization reached (near) full monomer conversion after 16 h of irradiation with visible light, yielding PMA with an M_n of 8290 Da and a \bar{D} of 1.07 (Table 1, entry 5). Similar results were obtained when an alternative TTC compound, 2-(((butylthio)carbonothiolyl)thio)propanoic acid (TTC-2), was employed (Table 1, entry 6; Figure S3), indicating the universality of the trithiocarbonate photoactivation mechanism. A curious feature of the present study is the difference in induction period between the two systems (i.e., UV and visible activation).

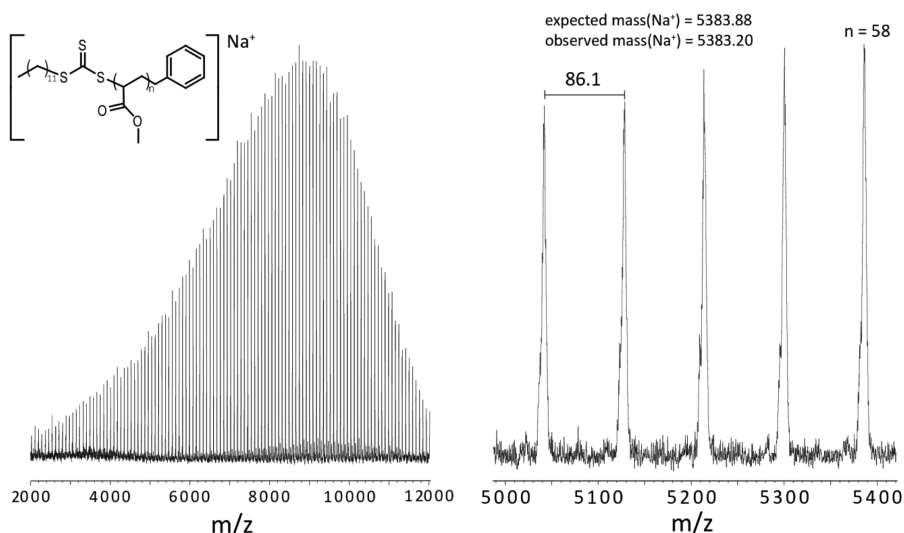


Figure 3. MALDI-ToF spectra of PMA homopolymer synthesized via visible light photocontrolled radical polymerization depicting single polymer species where the separation between peaks corresponds to the methyl acrylate monomer unit. The value of the observed mass is close to the expected mass of the targeted polymer structure, providing strong evidence for the retention of α and ω end-groups at high monomer conversions (ca. 93% in this case).

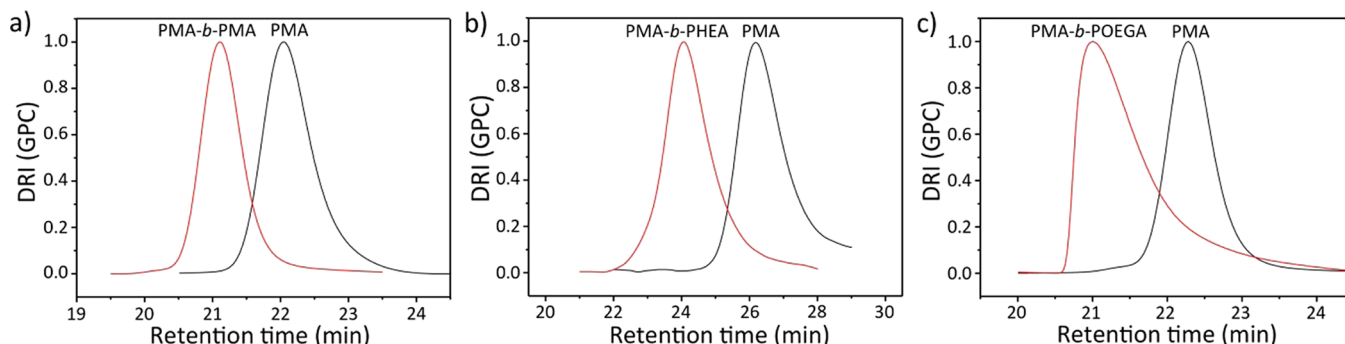


Figure 4. *In situ* chain extensions of PMA macroinitiator with different monomers. The targeted DP_n was 100 for each block. (a) PMA-*b*-PMA, (b) PMA-*b*-PHEA, and (c) PMA-*b*-POEGA.

Induction periods are commonly encountered in traditional RAFT reactions; however, their exact cause remains unclear.⁵⁹ It has been proposed that the induction period is due to slow initialization of the TTC species, whereby it is converted to a single monomer adduct prior to polymerization. In this case, the visible light process appears much slower at performing this transformation, perhaps due to the weaker absorption of energy in this wavelength region.

It was noticed that the visible light photoreactor warmed slightly to a temperature of $\sim 40^\circ\text{C}$ with extended irradiation times. To assess the effect of temperature, a control experiment was performed where the reaction mixture was heated at 60°C in the dark for 16 h. No polymerization was observed after 24 h (Table 1, entry 1), indicating that the polymerization was not thermally activated. Also, in the absence of a TTC species (i.e., monomer and solvent only) under the same irradiation conditions, no polymerization was observed (Table 1, entry 7), indicating self-initiation of monomer did not occur under the irradiation conditions. This is in direct contrast to the UV-activated polymerization, where self-initiation of methyl acrylate is known to occur,²¹ and was observed in the current work by the formation of an insoluble gel after 16 h UV irradiation (Table 1, entry 4). These control experiments crucially verified that the formed PMA was indeed due to photoactivation of the

trithiocarbonate under visible light irradiation and also demonstrate the advantage of using visible light mediated pathways compared to higher energy (i.e., UV) activation in photopolymerization processes by, in this case, avoiding self-initiation.

The PMA synthesized under visible light irradiation displayed excellent retention of α and ω end-groups even at (near) full monomer conversion, as evidenced by MALDI-ToF and ^1H NMR analysis. The MALDI-ToF spectrum shows a single monomodal series, providing strong evidence for the near-quantitative retention of α and ω end-groups at high monomer conversions (Figure 3). Furthermore, using peak area integration of the recorded ^1H NMR spectra, close agreement between all expected proton signal peak areas were observed when either TTC was employed (Figure S4).

To further confirm the end-group fidelity of the polymer structure, a chain extension experiment was performed to generate a pseudodiblock copolymer PMA-*b*-PMA in a one-pot fashion. The GPC differential refractive index (DRI) chromatogram of the chain extended product showed a clean shift toward lower retention times, indicating the formation of higher molecular weight species (Figure 4a). In addition, no low molecular weight tailing was observed, and the chain extended product has a D value of 1.05. Additional chain

extension experiments were performed with *in situ* formed PMA macroinitiators using 2-hydroxyethyl acrylate (HEA) and oligo(ethylene glycol) methyl ether acrylate (OEGA) monomers to yield well-defined amphiphilic diblock copolymers with similar efficiency (Figure 4b,c). The tail observed for the diblock copolymer PMA-*b*-POEGA may be due to column interactions with the graft-like OEG side chains. Regardless, the successful reinitiation of the PMA macroinitiator was evident for all cases.

Multiblock Copolymers via Sequential Chain Extensions in One Pot. The microstructural integrity (in particular, the α and ω chain-end fidelities) of synthetic polymers has become increasingly important, especially for enabling the efficient synthesis of sequence-defined multiblock copolymers,^{60–64} polymer chain encoding applications,^{65,66} or postpolymerization end-group modifications.⁶⁷ The observed excellent chemical fidelity of the formed polymers under visible light photoactivation as well as the successful chain extension experiments shown by the synthesis of diblock copolymers gave us the impetus to prepare higher order multiblock copolymers in a one-pot fashion.^{28,64,68} For this, we have synthesized a pseudohexablock (PMA-*b*-PMA-*b*-PMA-*b*-PMA-*b*-PMA) copolymer, targeting high monomer conversions (>90%) and high number-averaged degree of polymerization (DP_n) of 100 for each block. The resultant GPC DRI chromatograms of the polymers after each chain extension were monomodal (with $\bar{D} < 1.15$) and show minimal tailing toward lower molecular species, demonstrating an outstanding level of control throughout the entire polymerization (Figure 5a,b). However, the emergence of a high molecular weight shoulder with increasing block number was evident. This is attributed to bimolecular termination events and is believed to

be enhanced by the high viscosities of the reaction mixture, which increase with increasing molecular weight of the multiblock copolymer (i.e., with each chain extension). The high molecular weight shoulder peaks led to higher experimental M_n values compared to the theoretical ones, thus exaggerating the discrepancy as the shoulder grew larger (Figure 5b). The termination events may potentially be minimized through optimization of the reaction conditions. Nevertheless, considering the challenges of synthesizing well-defined high molecular weight block copolymers in a one-pot fashion,⁶⁹ the current photopolymerization system proved extremely efficient, with ≤ 24 h of irradiation time required to reach $\geq 92\%$ monomer conversion for each chain extension step (Table S1, entries 6–11). Furthermore, this system eliminates the risk of having exogenous (photo)initiators that can compromise the microstructural integrity of the polymer chain,⁷⁰ theoretically allowing for quantitative chain-end functionality.^{9,36}

Extension to Other Solvent Systems and Acrylamides.

As the initial studies were conducted using a polar organic solvent (DMSO), it was of interest to ascertain if the system is as effective in other solvents. A variety of solvents of varying polarities such as dimethylformamide (DMF), toluene, and acetone were tried and shown to be suitable for the polymerization of MA (Table 2, entries 1–3). The differences in solvent polarity appear to have a negligible effect on the polymerization rate, while the molecular weight distributions of the furnished PMA products are almost identical (Figure S5). By using a nonpolar solvent like toluene, we have also demonstrated the successful preparation of poly(*tert*-butyl acrylate) (PtBA) ($\bar{D} = 1.06$), which has poor solubility in DMSO (Table 2, entry 4). Furthermore, we also investigated the possibility of applying the visible light photopolymerization system to polymerize acrylamides under aqueous conditions. Polymerization of *N*-isopropylacrylamide (NIPAM) in aqueous solution was readily achieved (Table 2, entry 5), with 20% v/v of dioxane needed to help solubilize the TTC.⁶⁹ Using water as a polymerization medium can have many advantages such as low cost, environmentally friendly, and permitting the synthesis of biorelevant polymers.^{46,71–73} The formation of PNIPAM of differing molecular weights was achieved by changing the targeted DP_n and allowing the reaction to proceed to high monomer conversions. Three different sizes of PNIPAM polymers were prepared with excellent agreement between the targeted molecular weights and those observed via GPC (Figure 6 and Table 2, entries 5–7). The irradiation times required to reach high monomer conversions increase for larger targeted DP_n values, believed to be due to a lower radical concentration in solution as a result of the lower concentration of photoactive TTC species. The GPC DRI chromatograms of all PNIPAM products were monomodal and symmetrical, indicating that the photopolymerizations were still well-controlled even for the synthesis of high molecular weight polymers and at extended irradiation times. The ability to perform the reaction in different solvents opens avenues for the polymerization of a wide range of monomer types (e.g., hydrophobic, hydrophilic) as long as the TTC and monomer are soluble in the employed solvent (mixture).

Synthesis of Network Hydrogel via Visible Light Photocontrolled Radical Polymerization. Interest in controlled polymer network formation has surged recently due to the growing potential for gel-like materials in high-tech applications such as chromatographic separation media,⁷⁴ drug-

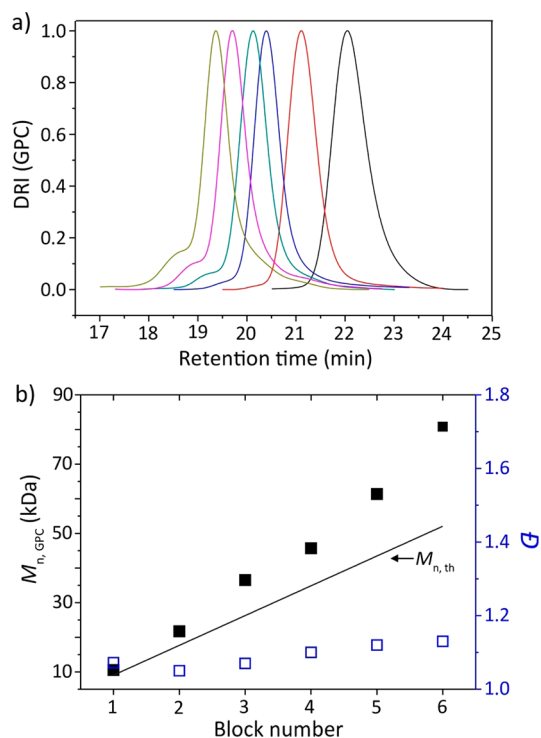
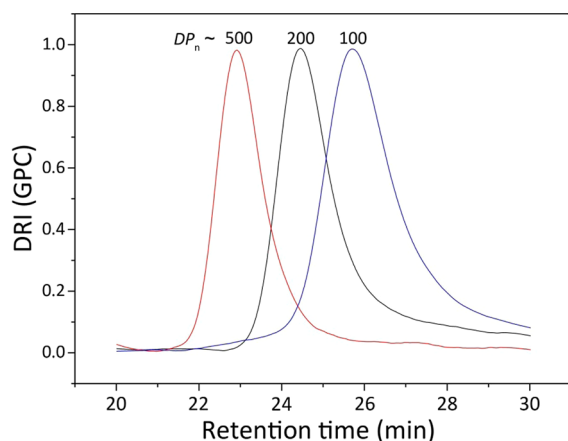


Figure 5. (a) GPC DRI chromatograms following each chain extension for the linear pseudohexablock (PMA-*b*-PMA-*b*-PMA-*b*-PMA-*b*-PMA) copolymer with a targeted DP_n of 100 per block. (b) M_n and \bar{D} values obtained via GPC analysis.

Table 2. Experimental Conditions and Characterization Data for Homopolymers Synthesized Using Different Monomers and/or Solvent Systems via Visible Light Mediated Photopolymerization

entry	monomer	light ^{a-c}	TTC ^{a-c}	solvent	[M] ₀ /[TTC] ₀	t (h)	% conv ^{a-c}	M _{n,th} (Da) ^{a-c}	M _{n,GPC} (Da) ^{a-c}	Đ ^{a-c}
1	MA	Vis	1	DMF	100	24	91	8200	9900	1.11
2	MA	Vis	1	toluene	100	24	95	8560	10160	1.12
3	MA	Vis	1	acetone	100	24	92	8290	10280	1.08
4	tBA	Vis	2	toluene	100	24	91	11670	10560	1.06
5	NIPAM	Vis	2	H ₂ O/dioxane ^f	100	20	>99	8760	9340	1.24 ^g
6	NIPAM	Vis	2	DMSO	200	24	85	19250	20490	1.19 ^g
7	NIPAM	Vis	2	DMSO	500	48	88	50030	55810	1.12 ^g

^{a-c}As for Table 1. ^fWater:1,4-dioxane solvent mixture (4:1 v/v ratio) used to ensure solubilization of TTC. ^gAnalysis performed on a GPC system using DMF (with 0.05 M LiBr added) as the eluent.

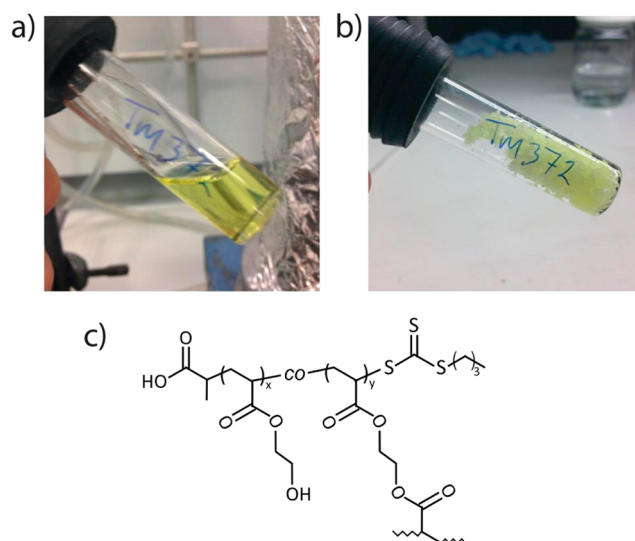
**Figure 6.** Overlay of GPC DRI chromatograms of the synthesized PNIPAM with different targeted DP_n values via visible light mediated photocontrolled radical polymerization.

delivery vehicles,^{75,76} biocoatings,^{77,78} and molecular imprinting.^{77,79} Free radical photoinduced gelation reactions have been used extensively in industry to create insoluble resins and cross-linked polymer networks,⁸⁰ where UV irradiation has been predominantly used to create such structures. Further in this study, the visible light photoactivation of TTCs was used to create network gels through a photocontrolled radical polymerization process. Polymerization of a hydrophilic acrylate monomer HEA in the presence of a divinyl acrylate cross-linker (ethylene glycol diacrylate (EGDA)) and a model trithiocarbonate (TTC-2) in aqueous solution (water/dioxane (4:1 v/v)) produced a hydrogel after 16 h of visible light irradiation (Figure 7).

The resulting network gel was measured to have a swelling weight ratio (q_w) of 4.54 and a swelling degree percentage (%_{sd}) of 354%. The monomer and solvent versatility as well as the inclusion of the functional trithiocarbonate moiety within the network structure that is capable of undergoing several facile postpolymerization transformations⁸¹ means that a wide variety of network gels may be accessible via this technique.

CONCLUSIONS

In this study, the visible light mediated controlled radical polymerization of acrylates and acrylamides using solely trithiocarbonates (TTCs) as control agents (i.e., in the absence of any exogenous (photo)initiators or catalysts) was demonstrated. Through selective excitation of the $n \rightarrow \pi^*$ absorption band of common TTCs, polyacrylates and polyacrylamides of low dispersity and controllable molecular weights were attained. In addition, the absence of exogenous radical sources and

**Figure 7.** PHEA hydrogel formation ([HEA]:[EGDA]:[TTC-2] of 100/30/1 in water/dioxane (4:1 v/v) with monomer concentration set at 50 wt %). (a) Initial reaction mixture (i.e., $t = 0$). (b) Reaction mixture after 16 h irradiation with visible light. (c) Chemical structure of the cross-linked polymer network.

(metal) catalysts allows for the generation of well-controlled polymers of “ideal” purity that possess excellent retention of both α and ω end groups, as evidenced by MALDI-ToF MS and ¹H NMR analysis. This key feature has been exploited further in the one-pot synthesis of a high molecular weight pseudohexablock copolymer. Furthermore, this system is amenable to different solvents of varying polarities, including water. Given the many advantages of photocontrolled radical polymerization this technique will be highly beneficial for (bio)materials science applications such as surface patterning. The employment of this technique for the fabrication of novel materials will be reported in forthcoming publications.

ASSOCIATED CONTENT

Supporting Information

Additional characterization and experimental data. The Supporting Information is available free of charge on the ACS Publications website at DOI: 10.1021/acs.macromol.5b00965.

AUTHOR INFORMATION

Corresponding Author

*E-mail gregghq@unimelb.edu.au (G.G.Q.).

Notes

The authors declare no competing financial interest.

■ ACKNOWLEDGMENTS

The authors acknowledge Kyra Schwarz and Professor Ken Ghigginio from the Ultrafast and Microspectroscopy Laboratories Group, The University of Melbourne, for assistance with light source characterization. The authors also acknowledge financial support from the Australian Research Council via the Future Fellowship (FT110100411, G.G.Q.) scheme. T.M. is the recipient of an Australian Postgraduate Award (APA).

■ REFERENCES

- (1) Matyjaszewski, K.; Tsarevsky, N. V. *J. Am. Chem. Soc.* **2014**, *136*, 6513–6533.
- (2) Wang, J.-S.; Matyjaszewski, K. *J. Am. Chem. Soc.* **1995**, *117*, 5614–5615.
- (3) Kato, M.; Kamigaito, M.; Sawamoto, M.; Higashimura, T. *Macromolecules* **1995**, *28*, 1721–1723.
- (4) Percec, V.; Guliashevili, T.; Ladislav, J. S.; Wistrand, A.; Stjern Dahl, A.; Sienkowska, M. J.; Monteiro, M. J.; Sahoo, S. *J. Am. Chem. Soc.* **2006**, *128*, 14156–14165.
- (5) Rosen, B. M.; Percec, V. *Chem. Rev.* **2009**, *109*, 5069–5119.
- (6) Zhang, N.; Samanta, S. R.; Rosen, B. M.; Percec, V. *Chem. Rev.* **2014**, *114*, 5848–5958.
- (7) Hawker, C. J.; Bosman, A. W.; Harth, E. *Chem. Rev.* **2001**, *101*, 3661–3688.
- (8) Grubbs, R. B. *Polym. Rev.* **2011**, *51*, 104–137.
- (9) Moad, G.; Rizzardo, E.; Thang, S. H. *Acc. Chem. Res.* **2008**, *41*, 1133–1142.
- (10) Moad, G.; Rizzardo, E.; Thang, S. H. *Aust. J. Chem.* **2012**, *65*, 985–1076.
- (11) Stuart, M. A. C.; Huck, W. T.; Genzer, J.; Müller, M.; Ober, C.; Stamm, M.; Sukhorukov, G. B.; Szleifer, I.; Tsukruk, V. V.; Urban, M. *Nat. Mater.* **2010**, *9*, 101–113.
- (12) Matyjaszewski, K.; Müller, A. H. *Controlled and Living Polymerizations: From Mechanisms to Applications*; John Wiley & Sons: New York, 2009.
- (13) Leibfarth, F. A.; Mattson, K. M.; Fors, B. P.; Collins, H. A.; Hawker, C. J. *Angew. Chem., Int. Ed.* **2013**, *52*, 199–210.
- (14) Konkolewicz, D.; Schröder, K.; Buback, J.; Bernhard, S.; Matyjaszewski, K. *ACS Macro Lett.* **2012**, *1*, 1219–1223.
- (15) Magenau, A. J.; Bortolamei, N.; Frick, E.; Park, S.; Gennaro, A.; Matyjaszewski, K. *Macromolecules* **2013**, *46*, 4346–4353.
- (16) Xiao, P.; Zhang, J.; Dumur, F.; Tehfe, M. A.; Morlet-Savary, F.; Graff, B.; Gigmes, D.; Fouassier, J. P.; Lalevée, J. *Prog. Polym. Sci.* **2015**, *41*, 32–66.
- (17) Fors, B. P.; Hawker, C. J. *Angew. Chem., Int. Ed.* **2012**, *51*, 8850–8853.
- (18) Treat, N. J.; Fors, B. P.; Kramer, J. W.; Christianson, M.; Chiu, C.-Y.; Alaniz, J. R. d.; Hawker, C. J. *ACS Macro Lett.* **2014**, *5*, 580–584.
- (19) Poelma, J. E.; Fors, B. P.; Meyers, G. F.; Kramer, J. W.; Hawker, C. J. *Angew. Chem., Int. Ed.* **2013**, *52*, 6844–6848.
- (20) Fors, B. P.; Poelma, J. E.; Menyo, M. S.; Robb, M. J.; Spokoyny, D. M.; Kramer, J. W.; Waite, J. H.; Hawker, C. J. *J. Am. Chem. Soc.* **2013**, *135*, 14106–14109.
- (21) Anastasaki, A.; Nikolaou, V.; Zhang, Q.; Burns, J.; Samanta, S. R.; Waldron, C.; Haddleton, A. J.; McHale, R.; Fox, D.; Percec, V.; Wilson, P.; Haddleton, D. M. *J. Am. Chem. Soc.* **2013**, *136*, 1141–1149.
- (22) Zhang, T.; Chen, T.; Amin, I.; Jordan, R. *Polym. Chem.* **2014**, *5*, 4790–4796.
- (23) Ciftci, M.; Tasdelen, M. A.; Li, W.; Matyjaszewski, K.; Yagci, Y. *Macromolecules* **2013**, *46*, 9537–9543.
- (24) Yang, Q.; Dumur, F.; Morlet-Savary, F.; Poly, J.; Lalevée, J. *Macromolecules* **2015**, *48*, 1972–1980.
- (25) Shanmugam, S.; Xu, J.; Boyer, C. *Chem. Sci.* **2015**, *6*, 1341–1349.
- (26) Xu, J.; Shanmugam, S.; Duong, H.; Boyer, C. *Polym. Chem.* **2014**, Advance Article.
- (27) Xu, J.; Jung, K.; Corrigan, N. A.; Boyer, C. *Chem. Sci.* **2014**, *5*, 3568–3575.
- (28) Xu, J.; Jung, K.; Atme, A.; Shanmugam, S.; Boyer, C. *J. Am. Chem. Soc.* **2014**, *136*, 5508–5519.
- (29) Zhang, G.; Song, I. Y.; Ahn, K. H.; Park, T.; Choi, W. *Macromolecules* **2011**, *44*, 7594–7599.
- (30) Shao, J.; Huang, Y.; Fan, Q. *Polym. Chem.* **2014**, *5*, 4195–4210.
- (31) Lalevée, J.; Telitel, S.; Xiao, P.; Lepeltier, M.; Dumur, F.; Morlet-Savary, F.; Gigmes, D.; Fouassier, J.-P. *Beilstein J. Org. Chem.* **2014**, *10*, 863–876.
- (32) Otsu, T.; Yoshida, M. *Makromol. Chem., Rapid Commun.* **1982**, *3*, 127–132.
- (33) Otsu, T. *J. Polym. Sci., Part A: Polym. Chem.* **2000**, *38*, 2121–2136.
- (34) Otsu, T.; Matsunaga, T.; Kuriyama, A.; Yoshioka, M. *Eur. Polym. J.* **1989**, *25*, 643–650.
- (35) Wang, H.; Li, Q.; Dai, J.; Du, F.; Zheng, H.; Bai, R. *Macromolecules* **2013**, *46*, 2576–2582.
- (36) Zhou, H.; Johnson, J. A. *Angew. Chem., Int. Ed.* **2013**, *125*, 2291–2294.
- (37) Khan, M. Y.; Cho, M.-S.; Kwark, Y.-J. *Macromolecules* **2014**, *47*, 1929–1934.
- (38) Lalevée, J.; Blanchard, N.; El-Roz, M.; Allonas, X.; Fouassier, J.-P. *Macromolecules* **2008**, *41*, 2347–2352.
- (39) Quinn, J. F.; Davis, T. P.; Barner, L.; Barner-Kowollik, C. *Polymer* **2007**, *48*, 6467–6480.
- (40) Zard, S. Z. *Angew. Chem., Int. Ed.* **1997**, *36*, 672–685.
- (41) Coyle, J. D. *Tetrahedron* **1985**, *41*, 5393–5425.
- (42) Lu, L.; Zhang, H.; Yang, N.; Cai, Y. *Macromolecules* **2006**, *39*, 3770–3776.
- (43) Barton, D. H. R.; George, M. V.; Tomoeda, M. *J. Chem. Soc.* **1967**, 1967–1974.
- (44) Ajayaghosh, A.; Das, S.; George, M. V. *J. Polym. Sci., Part A: Polym. Chem.* **1993**, *31*, 653–659.
- (45) Tazhe Veetil, A.; Šolomek, T.; Ngoy, B. P.; Pavlíková, N.; Heger, D.; Klán, P. *J. Org. Chem.* **2011**, *76*, 8232–8242.
- (46) Shi, Y.; Gao, H.; Lu, L.; Cai, Y. *Chem. Commun.* **2009**, 1368–1370.
- (47) Shi, Y.; Liu, G.; Gao, H.; Lu, L.; Cai, Y. *Macromolecules* **2009**, *42*, 3917–3926.
- (48) Lu, L.; Yang, N.; Cai, Y. *Chem. Commun.* **2005**, 5287–5288.
- (49) Jiang, W.; Lu, L.; Cai, Y. *Macromol. Rapid Commun.* **2007**, *28*, 725–728.
- (50) Ham, M. k.; HoYouk, J.; Kwon, Y. K.; Kwark, Y. J. *J. Polym. Sci., Part A: Polym. Chem.* **2012**, *50*, 2389–2397.
- (51) Zhang, J.; Li, A.; Liu, H.; Yang, D.; Liu, J. *J. Polym. Sci., Part A: Polym. Chem.* **2014**, *52*, 2715–2724.
- (52) Liu, G.; Shi, H.; Cui, Y.; Tong, J.; Zhao, Y.; Wang, D.; Cai, Y. *Polym. Chem.* **2013**, *4*, 1176–1182.
- (53) Tong, J.; Shi, Y.; Liu, G.; Huang, T.; Xu, N.; Zhu, Z.; Cai, Y. *Macromol. Rapid Commun.* **2013**, 1827–1834.
- (54) Narayanam, J. M.; Stephenson, C. R. *Chem. Soc. Rev.* **2011**, *40*, 102–113.
- (55) Prier, C. K.; Rankic, D. A.; MacMillan, D. W. *Chem. Rev.* **2013**, *113*, 5322–5363.
- (56) Schultz, D. M.; Yoon, T. P. *Science* **2014**, *343*, 1239176.
- (57) Ciamician, G. *Science* **1912**, *36*, 385–394.
- (58) Wong, E. H. H.; Lam, S. J.; Nam, E.; Qiao, G. G. *ACS Macro Lett.* **2014**, *3*, 524–528.
- (59) Moad, G. *Macromol. Chem. Phys.* **2014**, *215*, 9–26.
- (60) Gody, G.; Maschmeyer, T.; Zetterlund, P. B.; Perrier, S. *Nat. Commun.* **2013**, *4*, 2505.
- (61) Gody, G.; Maschmeyer, T.; Zetterlund, P. B.; Perrier, S. *Macromolecules* **2014**, *47*, 639–649.
- (62) Soeriyadi, A. H.; Boyer, C.; Nystrom, F.; Zetterlund, P. B.; Whittaker, M. R. *J. Am. Chem. Soc.* **2011**, *133*, 11128–11131.

- (63) Zhang, Q.; Collins, J.; Anastasaki, A.; Wallis, R.; Mitchell, D. A.; Becer, C. R.; Haddleton, D. M. *Angew. Chem., Int. Ed.* **2013**, *125*, 4531–4535.
- (64) Anastasaki, A.; Nikolaou, V.; Pappas, G. S.; Zhang, Q.; Wan, C.; Wilson, P.; Davis, T. P.; Whittaker, M. R.; Haddleton, D. *Chem. Sci.* **2014**, *5*, 3536–3542.
- (65) Ouchi, M.; Badi, N.; Lutz, J.-F.; Sawamoto, M. *Nat. Chem.* **2011**, *3*, 917–924.
- (66) Chan-Seng, D.; Zamfir, M.; Lutz, J. F. *Angew. Chem., Int. Ed.* **2012**, *51*, 12254–12257.
- (67) Gauthier, M. A.; Gibson, M. I.; Klok, H.-A. *Angew. Chem., Int. Ed.* **2009**, *48*, 48–58.
- (68) Anastasaki, A.; Waldron, C.; Wilson, P.; Boyer, C.; Zetterlund, P. B.; Whittaker, M. R.; Haddleton, D. *ACS Macro Lett.* **2013**, 896–900.
- (69) Gody, G.; Maschmeyer, T.; Zetterlund, P. B.; Perrier, S. b. *Macromolecules* **2014**, *47*, 3451–3460.
- (70) Vandenberg, J.; Junkers, T. *Macromolecules* **2014**, *47*, 5051–5059.
- (71) Cunningham, M. F. *Prog. Polym. Sci.* **2008**, *33*, 365–398.
- (72) Liu, G.; Qiu, Q.; Shen, W.; An, Z. *Macromolecules* **2011**, *44*, 5237–5245.
- (73) Simakova, A.; Averick, S. E.; Konkolewicz, D.; Matyjaszewski, K. *Macromolecules* **2012**, *45*, 6371–6379.
- (74) Turson, M.; Zhou, M.; Jiang, P.; Dong, X. *J. Sep. Sci.* **2011**, *34*, 127–134.
- (75) Raghupathi, K.; Li, L.; Ventura, J.; Jennings, M.; Thayumanavan, S. *Polym. Chem.* **2014**, *5*, 1737–1742.
- (76) Peppas, N. A. *Curr. Opin. Colloid Interface Sci.* **1997**, *2*, 531–537.
- (77) Guntari, S. N.; Wong, E. H. H.; Goh, T. K.; Chandrawati, R.; Blencowe, A.; Caruso, F.; Qiao, G. G. *Biomacromolecules* **2013**, *14*, 2477–2483.
- (78) Sidorenko, A.; Krupenkin, T.; Aizenberg, J. *J. Mater. Chem.* **2008**, *18*, 3841–3846.
- (79) Gonzato, C.; Pasetto, P.; Bedoui, F.; Mazeran, P.-E.; Haupt, K. *Polym. Chem.* **2014**, *5*, 1313–1322.
- (80) Andrzejewska, E.; Bogacki, M. B.; Andrzejewski, M.; Janaszczyk, M. *Phys. Chem. Chem. Phys.* **2003**, *5*, 2635–2642.
- (81) Moad, G.; Rizzardo, E.; Thang, S. H. *Polym. Int.* **2011**, *60*, 9–25.